



RESEARCH PAPER

Modulation of *Arabidopsis* and monocot root architecture by CLAVATA3/EMBRYO SURROUNDING REGION 26 peptide

Nathan Czyzewicz¹, Chun-Lin Shi², Lam Dai Vu^{3,4,5,6}, Brigitte Van De Cotte^{3,4}, Charlie Hodgman⁷, Melinka A. Butenko² and Ive De Smet^{1,3,4,7,*}

¹ Division of Plant and Crop Sciences, School of Biosciences, University of Nottingham, Leicestershire LE12 5RD, UK

² Department of Biosciences, Section for Genetics and Evolutionary Biology, University of Oslo, N-0316 Oslo, Norway

³ Department of Plant Systems Biology, VIB, B-9052 Ghent, Belgium

⁴ Department of Plant Biotechnology and Genetics, Ghent University, B-9052 Ghent, Belgium

⁵ Department of Medical Protein Research, VIB, B-9000 Ghent, Belgium

⁶ Department of Biochemistry, Ghent University, B-9000 Ghent, Belgium

⁷ Centre for Plant Integrative Biology, School of Biosciences, University of Nottingham, Leicestershire LE12 5RD, UK

*To whom the correspondence should be addressed. E-mail: ive.desmet@psb.vib-ugent.be

Received 1 April 2015; Revised 1 June 2015; Accepted 26 June 2015

Editor: Ruediger Simon

Abstract

Plant roots are important for a wide range of processes, including nutrient and water uptake, anchoring and mechanical support, storage functions, and as the major interface with the soil environment. Several small signalling peptides and receptor kinases have been shown to affect primary root growth, but very little is known about their role in lateral root development. In this context, the CLE family, a group of small signalling peptides that has been shown to affect a wide range of developmental processes, were the focus of this study. Here, the expression pattern during lateral root initiation for several CLE family members is explored and to what extent CLE1, CLE4, CLE7, CLE26, and CLE27, which show specific expression patterns in the root, are involved in regulating root architecture in *Arabidopsis thaliana* is assessed. Using chemically synthesized peptide variants, it was found that CLE26 plays an important role in regulating *A. thaliana* root architecture and interacts with auxin signalling. In addition, through alanine scanning and *in silico* structural modelling, key residues in the CLE26 peptide sequence that affect its activity are pinpointed. Finally, some interesting similarities and differences regarding the role of CLE26 in regulating monocot root architecture are presented.

Key words: *Arabidopsis thaliana*, auxin, *Brachypodium distachyon*, CLE26, root, wheat.

Introduction

A small number of phytohormones have an impact on plant growth and development (Vanstraelen and Benkova, 2012; Davière and Achard, 2013; El-Showk *et al.*, 2013; Yoon and Kieber, 2013), but how this small number of chemical mediators can modulate the large number of physiological and

biochemical responses required during growth and development remains an open question. Lately, however, it has become apparent that small signalling peptides provide an additional layer of control to steer growth and development (Murphy *et al.*, 2012; Czyzewicz *et al.*, 2013; Murphy and De Smet,

2014). Small signalling peptides generally range in size between four and 75 amino acid residues and most—but not all—are cleavage products from precursor peptides (Murphy *et al.*, 2012; Czyzewicz *et al.*, 2013). Several of these precursors are post-translationally modified prior to cleavage, and this post-translational modification can be critical for peptide activity and binding affinity for their receptor partners (Butenko *et al.*, 2009, 2014; Matsuzaki *et al.*, 2010; Matsubayashi, 2011; Murphy *et al.*, 2012; Shinohara and Matsubayashi, 2013).

The CLV3/EMBRYO SURROUNDING REGION (ESR)-related (CLE) peptide family is an ancient group of signalling peptides that has been shown to affect a wide range of developmental processes (Strabala *et al.*, 2006; Miyawaki *et al.*, 2013). The *Arabidopsis thaliana* CLE family is comprised of 32 peptides, each consisting of 12–13 amino acids, and containing a CLV3/ESR consensus sequence (Strabala *et al.*, 2006; Betsuyaku *et al.*, 2011). These CLE peptides are products of a larger precursor protein, which is translated and post-translationally modified prior to cleavage. However, only a few of the CLE peptides have been functionally characterized, and for most it is unknown which receptor(s) mediate(s) their signal (Strabala *et al.*, 2006; Shinohara and Matsubayashi, 2013). CLV3, the founding member of the CLE family, is perhaps the best characterized of the CLE peptides and exerts a crucial function as a mobile signal controlling the size of the *A. thaliana* shoot apical meristem (Clark *et al.*, 1995; Fletcher *et al.*, 1999; Ogawa *et al.*, 2008; Ohyama *et al.*, 2009; Shinohara and Matsubayashi, 2013). Since mature CLE peptides display a high degree of redundancy with known receptors (Strabala *et al.*, 2006; Wang and Fiers, 2010), it is likely that strict tissue-specific control of expression and/or the formation of co-receptor complexes provides signalling specificity. An example of this redundancy is seen for CLV3, CLE19, and CLE40, which all trigger consumption of the root apical meristem in *A. thaliana*, resulting in a short root phenotype, but only CLE40 is actually expressed in the root apical meristem (Hobe *et al.*, 2003). The CLV3, CLE19, and CLE40 peptides all show an effect on the root meristem through a CLAVATA2 (CLV2)-dependent pathway (Fiers *et al.*, 2005), while CLV3 and CLE40 require CLV1 as part of a receptor complex to initiate the downstream signalling cascade (Ohyama *et al.*, 2009; Stahl *et al.*, 2013).

In land plants, the correct development of root architecture is vital for maximum uptake of water and minerals for growth. Root architecture differs greatly between species and can also be highly dynamic within a species if subjected to biotic or abiotic stress (Smith and De Smet, 2012). In addition to controlling primary root growth, developing lateral roots is another strategy which allows the plant to maximize the area over which nutrients are absorbed, and further allows the plant to anchor itself more firmly in the soil (Smith and De Smet, 2012). Lateral root primordia are formed from ~3 pairs of xylem pole pericycle cells from distinct cell files, which are primed by exposure to auxin in the basal meristem (Kurup *et al.*, 2005; De Smet *et al.*, 2007). Upon further exposure to auxin in the differentiation zone, the nuclei of these primed cells move toward a central point, and the cells divide

asymmetrically to form two central small daughter cells, and two distal large daughter cells—the stage 1 primordium (De Smet *et al.*, 2007). These cells divide asymmetrically in a strictly regulated manner through seven further stages, during which the primordium pushes through the endodermis, epidermis, and cortex, and becomes the emerged lateral root (Péret *et al.*, 2009; Lavenus *et al.*, 2013).

Here, CLE peptides, which—based on their expression profile—are likely candidates for regulating root architecture, were identified. To explore further their *in vivo* involvement in root development, their root growth response to synthetic peptide treatment was assessed. Based on the results, one member of the CLE family, namely CLE26, subsequently became the focus of the study, and its function and relationship to auxin signalling and response in *A. thaliana* were explored. By employing CLE26 peptide treatment on roots of *Brachypodium distachyon* and wheat, to what level there is functional conservation between *A. thaliana* and monocots was also investigated.

Materials and methods

Plant lines

A. thaliana lines expressing the β -glucuronidase gene (*GUS*) under the control of *CLE* peptide promoters were obtained from the Nottingham Arabidopsis Stock Centre (NASC) and/or provided by Jennifer Fletcher (Jun *et al.*, 2010) (Supplementary Table S1 available at *JXB* online). The following previously published lines were used: *arf7 arf19* (Okushima *et al.*, 2007), *pDR5::GUS* (De Smet *et al.*, 2007), *35S::DII:VENUS* (Brunoud *et al.*, 2012; Vernoux *et al.*, 2011), and *pPIN1::PIN1:GFP* (Benková *et al.*, 2003). The *cle26-1* (N689781) SALK T-DNA line was genotyped by PCR using primers designed by the T-DNA Primer Design Tool (signal.salk.edu) (*cle26-1* Forward, ACCCATTTTGIGTTTTTGCAC; *cle26-1* Reverse, ATTATACGCGTGGACCACTTG; and SALK LBb, ATTTTGCCGATTTTCGGAAC) and using the following PCR conditions: 94 °C 5 min, 40× (94 °C 30 s, 60 °C 30 s, 72 °C 1 min), 72 °C 5 min.

Growth conditions

A. thaliana and *B. distachyon* seeds were surface sterilized by immersion in 70% ethanol for 30 s, followed by immersion in 25% bleach for 20 min, and were then vernalized at 4 °C. The *A. thaliana* seedlings were grown at 20–22 °C, with 24 h daylight under fluorescent lamps [150 μM (m^2)⁻¹ min⁻¹] on 12 × 12 cm square Petri dishes containing 50 ml of half-strength Murashige and Skoog (1/2 MS) agar [2.154 g of MS medium (Duchefa), 0.1 g of myo-inositol (Sigma-Aldrich), 0.5 g of MES (Sigma-Aldrich) 1% (w/v) agar (Sigma) per litre of distilled water] containing the appropriate concentration of peptide diluted in water until 12 days after germination (DAG). Wheat seeds were surface sterilized by immersion in 5% hypochlorite for 15 min, before washing three times in water. Wheat and *B. distachyon* seedlings were grown at 20–22 °C, with 24 h daylight in 100 ml boiling tubes containing 20 ml of 1/2 MS agar with the appropriate concentration of peptide until 10–12 DAG. For GUS analyses, seedlings were grown at 20–22 °C, with 24 h daylight on 8 cm radius round Petri dishes containing 20 ml of 1/2 MS agar until 6 DAG. For quantitative PCR (qPCR) analyses, *A. thaliana* seedlings were grown at constant light conditions on 1/2 MS agar for 7 DAG and then transferred to 1 μM CLE26p for 24 h, or at 5 DAG to 1 μM 1-naphthaleneacetic acid (NAA). For green fluorescent protein (GFP) studies, seeds were surface sterilized by immersion in 70% ethanol for 30 s, followed by 20 min immersion in 20% bleach (final concentration

1% hypochlorite). Sterilized seeds were washed three times in sterile distilled water, before vernalizing for 24h at 4 °C. Sterile, vernalized seeds were germinated and grown on 1/2 MS medium [0.01% myo-inositol (Sigma-Aldrich), 0.05% MES (Sigma-Aldrich), and 1% (w/v) agar] until 5 DAG.

Synthetic peptides

Synthetic peptides were ordered from GenScript (www.genscript.com/) and were used at the following purities: CLE1/4p (98.8% or 98.2%), CLE7p (94.8% or 88.9%), CLE27p (71.2% or 73.6%), CLE26p (94.2, 89.6, 84.6, or 99.7%), mCLE26p 1A (92.1%), mCLE26p 2A (91.6%), mCLE26p 3A (99.4%), mCLE26p 4A (98.2%), mCLE26p 5A (98.6%), mCLE26p 6A (84.9%), mCLE26p 7A (94.3%), mCLE26p 8A (99.1%), mCLE26p 10A (97.5%), mCLE26p 11A (94.3%), and mCLE26p 12A (94.7%). All peptides used were diluted to a 10mM stock solution, correcting for purity [volume required for 10 mM×(purity/100)], and sequentially diluted to working concentrations prior to use. Stock and working solutions were stored at −20 °C.

Root architecture measurements

Emerged *A. thaliana* or *B. distachyon* lateral roots were counted using a dissection microscope. *B. distachyon* was removed from agar tubes by heating in a 95 °C water bath until the agar was melted, and mounted in 12×12cm plates in sterile, distilled water prior to analysis. Photos of the plates were taken using a digital camera mounted on a fixed stand before and after counting lateral roots. Primary root length and lateral root numbers were measured by use of FIJI (Schindelin *et al.*, 2012) and analysed in Excel. Lateral root density was calculated as the total number of emerged lateral roots/total primary root length.

GUS screening

Seedlings at 10–12 DAG were stained in GUS staining solution (0.05M sodium phosphate buffer, 5mM potassium ferrocyanide, 5mM potassium ferricyanide, 1mM 5-bromo-4-chloro-3-indolyl-β-D-glucuronide) until the stain was visible under a dissection microscope, before stopping the reaction by immersion in 70% ethanol for 5min. The seedlings were then cleared by incubation in acidified methanol [20% (v/v) methanol, 4% (v/v) HCl] for 15min, followed by incubation in alkalized ethanol [60% (v/v) ethanol, 7% (w/v) NaOH]. The ethanol concentration was then gradually decreased by 15–20min incubations in each of 40, 20, and 10% ethanol, before storage and analysis of the expression pattern in distilled water (Malamy and Benfey, 1997). Stained seedlings were imaged using a Leica DMRB binocular microscope and Leica Application Suite (Leica). When necessary to improve figure quality, brightness and contrast of the images were modified using Photoshop and, in such cases, all related figures were treated the same.

GFP analysis

Seedlings grown in the presence of CLE26p or 5-day-old seedlings transferred to fresh plates containing CLE26p were analysed by confocal microscopy (Leica TCS SP5) at 5 DAG or at different time points (0, 6, and 24h), respectively.

RNA extraction, cDNA synthesis, and (q)RT-PCR analysis

Total RNA was isolated with Trizol reagent (Invitrogen) or by using the RNeasy Mini Plant Kit (Qiagen) according to the manufacturer's instructions. Poly(dT) cDNA was prepared from 2mg of total RNA with Superscript II/III reverse transcriptase (Invitrogen) and quantified on a LightCycler 480 apparatus (Roche Diagnostics) with the SYBR Green I Master kit (Roche Diagnostics) according to the manufacturer's instructions using gene-specific primers

(CLE26 FW 5'-ACCATTCCCTTCGTCTCCA-3' and CLE26 REV 5'-CGTCGTTCTTGAACCATCT-3'). Three biological repeats were performed on a pool of seedlings and all individual reactions were done in triplicate. Graphs show one representative analysis. Data were analysed with qBase (Hellemans *et al.*, 2007) and normalized to *EEF1α4* (*EEF1α4_FW* 5'-CTGGAGGTTTTGAGGCTGGTAT-3' and *EEF1α4_REV* 5'-CCAAGGGTGAAGCAAGAAGA-3') and/or *ARP7* (*ARP7_FW* 5'-ACTCTTCTTGATGGACAGGTG-3' and *ARP7_REV* 5'-CTCAACGATTCCATGCTCCT-3'). To detect CLE26.1 and CLE26.2 splice variants, RNA was extracted with RNeasy (Qiagen), cDNA was prepared with an iScript cDNA Synthesis Kit (Bio-Rad), and specific primers (CLE26_F ATGCGAAATAACCATCCCTTC and CLE26.2_AS TTATGCTCTTCTGGTGGTTCG or CLE26.1_AS TCATACAGAAACATCCAAGACACAT) were used for PCR [94 °C 3min, 40× (94 °C 30s, 55 °C 30s, 72 °C 1min), 72 °C 7min].

Genevestigator analyses

Genevestigator (www.genevestigator.com) was used to assess transcriptional regulation of *CLE* genes for which microarray probes are available, using settings with a fold change of 2 and a *P*-value of 0.05.

Phylogenetic analyses

Full-length *A. thaliana* CLE peptide precursor sequences were obtained from Uniprot for all known *A. thaliana* CLE peptides. These sequences were used to BLAST for similar sequences in *Zea mays*, *Oryza sativa*, *B. distachyon*, *Brassica rapa*, *Selaginella moellendorffii*, and *Physcomitrella patens* using Phytozome v9.1 (Goodstein *et al.*, 2011). The indicated sequences were aligned with *A. thaliana* CLE peptide precursors to identify the conserved CLE region, and phylogenetic trees were built in CLC Workbench using the 12–13 amino acid conserved domains. The mature 12 amino acid sequences from *A. thaliana* and *B. distachyon* were further used to create a Weblogo alignment using WebLogo3 (Crooks *et al.*, 2004).

Structure prediction

The precursor protein was submitted to PHYRE for standard tertiary structure prediction and analysis (www.sbg.bio.ic.ac.uk/phyre2) (Kelley and Sternberg, 2009). The predicted secondary structure, model ranking, and relevant extra figures are shown in the Supplementary data at JXB online. Rotamers of Arg5 and Asp8 (Dunbrack, 2002) were explored and structural figures produced using Chimera v.1.5.3 (Pettersen *et al.*, 2004).

Results and discussion

CLE peptide expression is regulated by hormones and environmental triggers

Root architecture is controlled by hormonal and environmental cues (Smith and De Smet, 2012; Tian *et al.*, 2014). For example, auxin positively regulates several aspects of lateral root initiation, primordium development, and emergence (De Smet, 2012; Lavenus *et al.*, 2013), and abscisic acid (ABA) is crucial for salt-regulated root growth dynamics and acts—for instance—on meristem activation (De Smet *et al.*, 2003; Ding and De Smet, 2013; Duan *et al.*, 2013). Also, in response to various nutrient deficiencies, the root system displays high plasticity (Gruber *et al.*, 2013; Tian *et al.*, 2014). It is therefore not unexpected that gene expression of factors regulating root architecture is under hormonal and environmental

control, and a number of reports suggest this to be the case for *CLE* expression. Specifically nitrate and phosphate appear to affect *CLE* expression strongly in various species during the regulation of root architecture and/or nodulation, as do cytokinin and gibberellin (Okamoto *et al.*, 2009; Funayama-Noguchi *et al.*, 2011; Reid *et al.*, 2011; Mortier *et al.*, 2012; Araya *et al.*, 2014; Bidadi *et al.*, 2014; Lim *et al.*, 2014). To assess comprehensively the influence of hormones, nutrients, and abiotic stresses on the regulation of *CLE* expression in *A. thaliana*, available microarray data sets were probed. The combined analysis for those *CLE* genes—for which data were available and focusing on hormones and environmental triggers that had a significant effect—is shown in Table 1. Strikingly, *CLE2* and *CLE6* were mainly down-regulated by hormones, nutrients, and stress, while *CLE12* was mainly up-regulated. *CLE3*, *CLE26*, *CLE27*, *CLE41*, *CLE44*, and *CLE46* showed variable responses to the selected stimuli. For example, *CLE26*, *CLE41*, and *CLE44* are down-regulated by salicylic acid, while ABA and auxin up-regulated *CLE27*, *CLE41*, and/or *CLE44*. In conclusion, it indeed appears that

environmental cues and hormone levels effect *CLE* expression, possibly during primary and lateral root growth and development. However, these global transcript data do not provide any information on where and when *CLE* genes relevant for root architecture are expressed.

Primary and lateral root *CLE* expression patterns in *A. thaliana*

The expression pattern for several *CLE* genes has been described previously (Sharma *et al.*, 2003; Geier *et al.*, 2008; Hirakawa *et al.*, 2008; Jun *et al.*, 2010; Depuydt *et al.*, 2013). However, to evaluate which *CLE* peptides might play a role in mediating *A. thaliana* root architecture comprehensively and comparably, the expression patterns of 20 *CLE* genes in the primary root tip and during lateral root development were profiled using previously published *pCLE::GUS* fusions (Jun *et al.*, 2010) under the growth conditions used here. This analysis revealed distinct expression patterns, both in the root tip and during early stages of lateral root development (Supplementary Figs S1–S4

Table 1. Hormonal and environmental control of *CLE* expression

	Hormones					
	Brassinosteroids	ABA	Auxin	Jasmonic acid	Salicylic acid	
<i>CLE2</i>	–	–	–			
<i>CLE3</i>						
<i>CLE6</i>	–					
<i>CLE12</i>		+	–	+		
<i>CLE26</i>					–	
<i>CLE27</i>			+			
<i>CLE41</i>		+			–	
<i>CLE44</i>		+	+		–	
<i>CLE46</i>						
	Nutrients					
	Glucose	Iron deficiency	Nitrate	Phosphate deficiency	Sulphur deficiency	
<i>CLE2</i>	–	–	+		–	
<i>CLE3</i>				+		
<i>CLE6</i>	–	–		–		
<i>CLE12</i>	+			+	+	
<i>CLE26</i>						
<i>CLE27</i>						
<i>CLE41</i>	+					
<i>CLE44</i>		+				
<i>CLE46</i>						
	Stresses					
	Anoxia	Cold	Drought	Heat	Hypoxia	Salt
<i>CLE2</i>				–	–	
<i>CLE3</i>						
<i>CLE6</i>	–	+	–	–	–	
<i>CLE12</i>		+	+			+
<i>CLE26</i>						
<i>CLE27</i>						
<i>CLE41</i>				–		
<i>CLE44</i>		+	–			
<i>CLE46</i>			+			

+, significant up-regulation; –, significant down-regulation.

at *JXB* online). The majority of the observations are in agreement with an earlier report (Jun *et al.*, 2010); however, expression of *pCLE3::GUS*, *pCLE16::GUS*, and *pCLE17::GUS* was not observed in the vasculature. Given that the expression of *CLE* genes can be subject to environmental control (Table 1), the differences in expression observed could potentially be due to variations in growth conditions.

Based on the observed *CLE* expression patterns, a subset of *CLEs* was used for further analyses. Expression of *pCLE6::GUS*, *pCLE22::GUS*, *pCLE25::GUS*, *pCLE26::GUS*, and *pCLE27::GUS* was observed in the basal meristem, with *CLE6*, *CLE22*, *CLE25*, and *CLE26* expression seemingly restricted to the stele and with *CLE26* being the most strongly expressed (Fig. 1A; Supplementary Fig. S1 at *JXB* online). The latter expression patterns may indicate a role in lateral root patterning via establishment of the vascular pattern and/or priming of pericycle cells (De Smet *et al.*, 2007; Parizot *et al.*, 2008, 2012). During the early stages of lateral root development, *pCLE27::GUS* was specifically expressed in the asymmetrically dividing pericycle cells (Fig. 1C). Based on this expression pattern (in the core of the lateral root initiation site), it was hypothesized that *CLE27* could be a positive regulator of early stages of lateral root development. In contrast, during lateral root initiation and development, *pCLE1::GUS*, *pCLE4::GUS*, and *pCLE7::GUS* were expressed in the vasculature and pericycle, but excluded from the developing primordium (Fig. 1D–F). Based on these expression patterns (excluded from the lateral root initiation site), it is hypothesized that these *CLEs* may be negative regulators of early stages of lateral root development.

Synthetic *CLE* peptides affect *A. thaliana* primary and lateral root growth and development

To characterize further the involvement of *CLE* genes with an interesting lateral root-associated expression pattern and/or a regulation by hormonal or environmental triggers, chemically synthesized *CLE* peptides (*CLEps*) corresponding to the predicted products of the respective *A. thaliana* *CLE* genes (*AtCLEp*, referred to as *CLEp*) were used. *CLE1p*, *CLE4p*, *CLE7p*, *CLE26p*, and *CLE27p* were selected but, since *CLE1* and *CLE4* have the same mature peptide sequence, they were

represented by one synthetic peptide (*CLE1/CLE4p*) (Fig. 2A). Based on their expression patterns, a repressive (*CLE1*, *CLE4*, and *CLE7*) or inductive effect on lateral root development (*CLE26* and *CLE27*) was hypothesized for the selected peptides. To test the biological activity of the chemically synthesized peptides, initially a high concentration (compared with likely normal physiological conditions) of 10 μ M *CLEp* was applied to wild-type *A. thaliana* seedlings. This revealed a significant effect of all assayed *CLE* peptides, namely decreased primary root length (between a 76% and 94% decrease), decreased lateral root number (between a 57% and 88% decrease), and increased lateral root density (between a 98% and 179% increase) (Fig. 2B–D; Supplementary Fig. S5 at *JXB* online). The decrease in primary root length was predictable, since overexpression of *CLE* genes or application of chemically synthesized *CLE* peptides often results in consumption of the root apical meristem and/or a short primary root, and is possibly a non-specific response to high concentrations of exogenously applied peptide (Casamitjana-Martinez *et al.*, 2003; Fiers *et al.*, 2005; Kinoshita *et al.*, 2007; Jun *et al.*, 2010; Depuydt *et al.*, 2013). In addition, the increased lateral root density by *CLE1*, *CLE4*, and *CLE7* is in contrast to the hypothesized effect, namely a decrease in lateral root development. It is, however, possible that the increased lateral root density is a consequence of the dramatically reduced primary root growth.

Subsequently, it was assessed whether these chemically synthesized *CLE* peptides also affected root architecture at a lower, more physiologically relevant concentration (10 nM). Analyses of *A. thaliana* seedlings grown on 10 nM *CLEp* revealed that only those seedlings grown on *CLE26p* displayed a significant 83% decrease in primary root length, a 72% decrease in lateral root number, and a 94% increase in lateral root density compared with the control (Fig. 2E–G; Supplementary Fig. S5 at *JXB* online). However, there was no obvious effect of *CLE1p*, *CLE4p*, and *CLE7p* on primary root length and neither did these seedlings display a reduced lateral root density. A dose–response analysis further indicated that *CLE26p* is able to restrict primary root growth and increase lateral root density in *A. thaliana* at a minimum concentration of 1 nM (Fig. 3A–C). This is a similar activity threshold to other peptides, such as, for example,

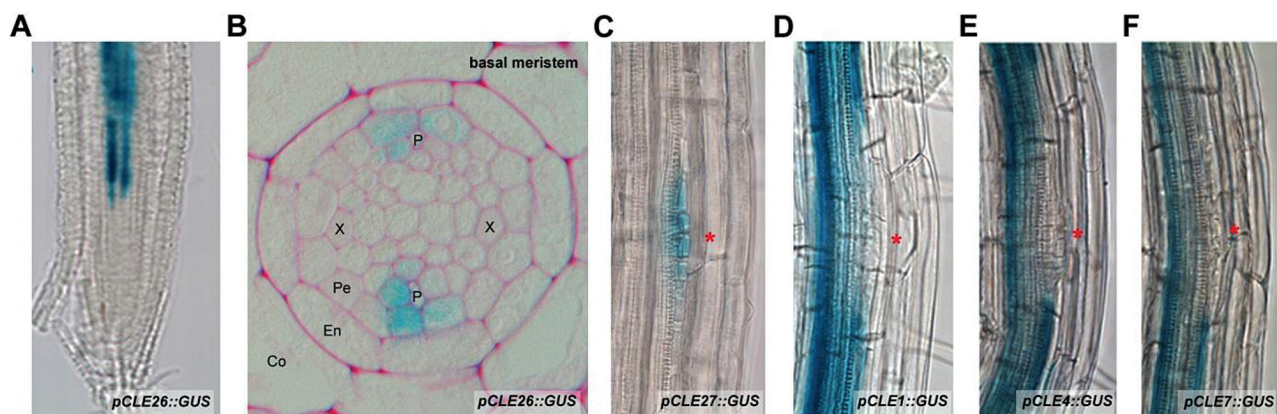


Fig. 1. *CLE* expression visualized through *pCLE::GUS* lines. (A, B) *pCLE26::GUS* in the primary root tip: (A) whole mount; (B) transverse section in the basal meristem. (C–F) *pCLE::GUS* during early stages of *A. thaliana* lateral root development: (C) *pCLE27::GUS*; (D) *pCLE1::GUS*; (E) *pCLE4::GUS*; (F) *pCLE7::GUS*. A red asterisk indicates the position of the lateral root primordium. Seedling age, 5–7 d after germination.

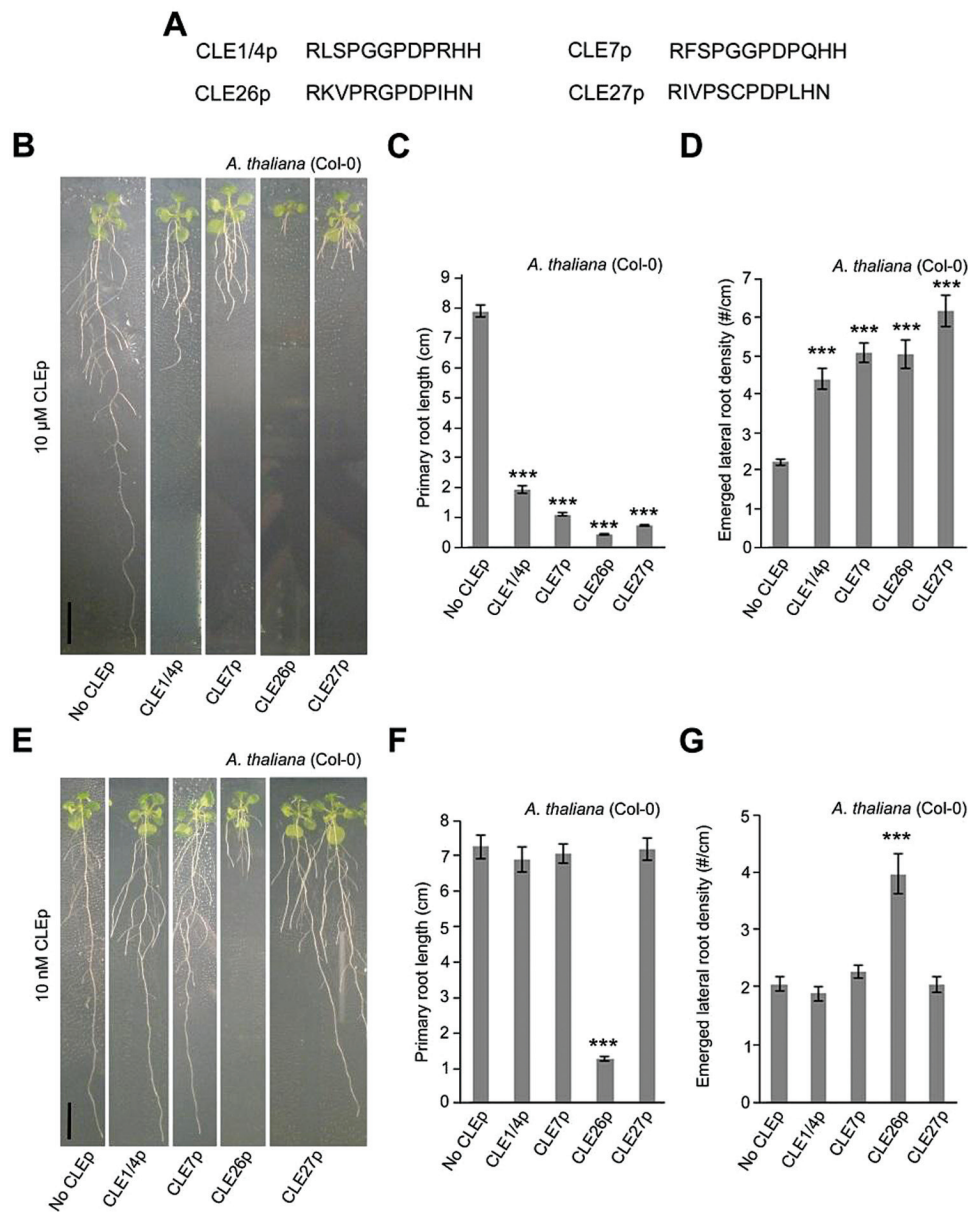


Fig. 2. CLE peptide treatment of *A. thaliana*. (A) Sequence of synthetic CLE peptides used. (B–G) Treatment of wild-type seedlings with 10 μ M (B, C) or 10 nM CLE peptide (E–G). Representative pictures of CLE26p-treated wild-type seedlings at 12 d after germination (B and E). Quantification of primary root length (C and F) and emerged lateral root density (D and G) for CLE26p-treated wild-type seedlings. The bar graphs indicate the mean \pm SE. Statistical significance (Student's *t*-test) compared with the no peptide treatment is indicated: ****P*<0.01. Scale bar=1 cm. (This figure is available in colour at *JXB* online.)

RALF, which is also active in the nanomolar range (Pearce *et al.*, 2001), and TDIF (CLE41/CLE44), which is active in the picomolar range (Sawa *et al.*, 2006). Surprisingly, the present CLE26p application data (at higher concentrations) are not in agreement with earlier observations based on overexpression of *CLE26* (Strabala *et al.*, 2006), but correspond to another report that showed that 19 CLE peptides are able to induce a short root phenotype (Kinoshita *et al.*, 2007). In agreement with the present results, the latter study also showed that among all CLE peptides tested, CLE26p is the most effective one in inducing the short-root phenotype in *A. thaliana*. Intriguingly, CLE26p resulted in a subtle, but significant, increase in primary root length at a concentration of 0.1 nM and 0.01 nM (Fig. 3B), and it is possible that the previously reported *CLE26* overexpression lines (which could

be mild overexpressors) (Strabala *et al.*, 2006) capture this. Taken together, the results suggest that CLE26 plays a role in *A. thaliana* primary and lateral root growth and development.

CLE26 is expressed at the phloem pole

To gain insight into the effect of CLE26p in relation to its expression pattern at cellular resolution, transverse root sections of *pCLE26::GUS* seedlings were analysed. This revealed that *CLE26* is expressed in the stele at the phloem pole (Fig. 1B), which is in agreement with a genome-wide expression profiling of xylem and phloem–cambium isolated from the root hypocotyl of *A. thaliana* where a phloem–cambium bias was reported (Zhao *et al.*, 2005). It was recently proposed that CLE45, BAM3, and BRX might interact to guide the proper

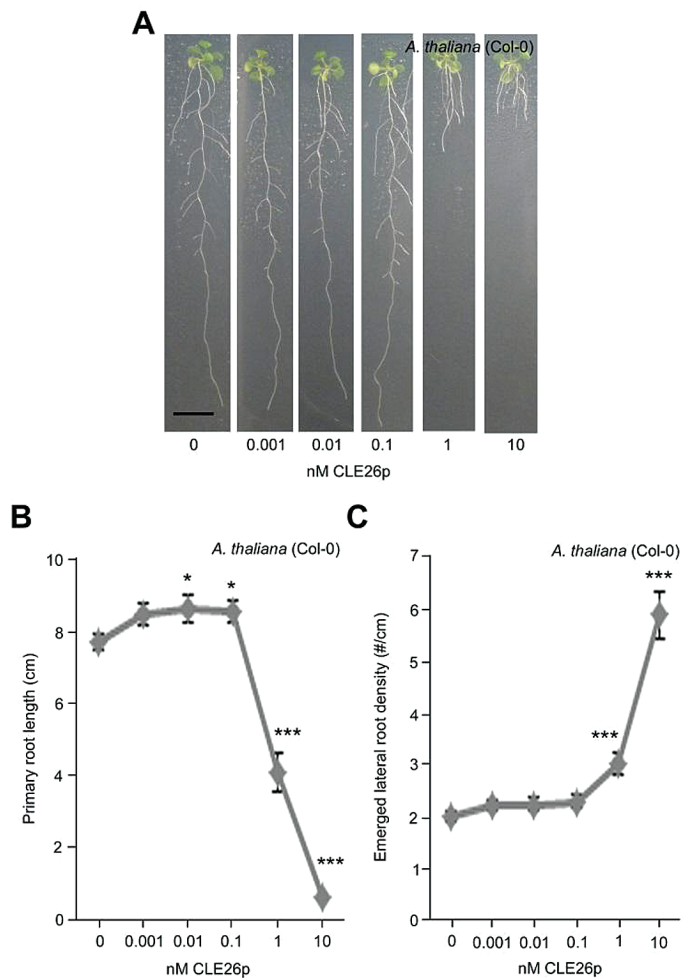


Fig. 3. CLE26p concentration gradient on *A. thaliana*. (A) Representative pictures of CLE26p-treated wild-type seedlings at 12 d after germination. (B, C) Quantification of primary root length (B) and emerged lateral root density (C) for CLE26p-treated wild-type seedlings. The graphs indicate the mean \pm SE. Statistical significance (Student's *t*-test) compared with no peptide treatment is indicated: *** $P < 0.01$; * $P < 0.05$. Scale bar=1 cm. (This figure is available in colour at *JXB* online.)

transition of protophloem cells from proliferation to differentiation, which could determine the growth capacity of the root meristem (Depuydt *et al.*, 2013; Rodriguez-Villalon *et al.*, 2014), and it is possible that CLE26 has a similar function. To support this, fewer cells expressing the protophloem marker *pAT2G18380::GFP* (S32; Lee *et al.*, 2006) were observed in CLE26p-treated root tips (Supplementary Fig. S6 at *JXB* online). It is, however, unlikely that CLE26 signals through the same pathway as CLE45 as a *bam3* mutant is equally sensitive to CLE26 as the wild type (Depuydt *et al.*, 2013), ruling out BAM3 as a putative CLE26 receptor. However, CLE26 displayed similar strong binding affinity for BAM1 and BAM2, and moderate affinity for CLV1 and CLV2 (Guo *et al.*, 2010), making these receptors good candidates for mediating the CLE26 phenotype.

CLE26 peptide sequence–activity analyses identify key amino acids

Given that application of low—possibly physiologically more relevant—concentrations of CLE26p gave a reduction in

primary root length and an increase in lateral root density, it was decided to focus on CLE26p for a more in-depth analysis of the sequence–activity relationship. To identify amino acids critical for CLE26p function, an alanine scan was performed using primary root length and lateral root density as biological assays (Fig. 4A–D; Supplementary Fig. S5 at *JXB* online). Seedlings grown on media containing 10 μ M mCLE26p^{R1A}, mCLE26p^{P4A}, mCLE26p^{R5A}, mCLE26p^{G6A}, mCLE26p^{D8A}, mCLE26p^{P9A}, mCLE26p^{I10A}, mCLE26p^{H11A}, and mCLE26p^{N12A} showed no significant decrease in primary root length compared with untreated *A. thaliana*, and were significantly different from non-mutated CLE26p treatment (Fig. 4C). The total number of emerged lateral roots was similarly not decreased for these mCLE26p variants compared with the CLE26p control treatment (Supplementary Fig. S5). This suggested that these amino acid residues are critical for CLE26 function. In contrast, amino acid residues 2 and 3 do not appear to be critical for CLE function, since mCLE26p^{K2A} and mCLE26p^{V3A} displayed the same, but a less strong effect on primary root length as the non-mutated CLE26p variant (a decrease of between 52% and 63%) (Fig. 4C). Interestingly, mCLE26p^{P7A} displayed increased activity, with respect to both primary root length (a further decrease of 11%) and lateral root density (a further increase of 32%), compared with wild-type CLE26p (Fig. 4C, D). Finally, mCLE26p^{D8A} resulted in a slightly longer root than untreated seedling roots, but did not have an effect on lateral root density (Fig. 4C, D). Taken together, the series of alanine-substituted CLE26 peptides revealed several amino acids which are critical for bioactivity of CLE26, and pinpointed mCLE26p^{P7A} and mCLE26p^{D8A} as a hyperactive and a possible antagonistic peptide, respectively. Previous analyses of critical amino acid residues in, for example, CLE41/CLE44 [also referred to as TRACHEARY ELEMENT DIFFERENTIATION INHIBITORY FACTOR (TDIF)] (Ito *et al.*, 2006) and CLV3 (Kondo *et al.*, 2008) identified similar amino acids that are important for the peptide to have the required bioactivity.

Structural modelling of CLE26p explains the mCLE26p^{P7A} effect

CLE26 has similar residues at the N- and C-termini as CLV3 that are critical for correct function in *A. thaliana*, and mutation of more central amino acids causes a similar reduction in bioactivity to that reported for CLV3 (Kondo *et al.*, 2008) (Fig. 5A). That these amino acids are critical for function indicates that they contribute to the correct conformation for ligand–receptor interaction. Structural analysis of CLE26 indicates that Gly6 and Pro7 form the sharp bend of a hairpin, potentially putting the proteolytic cleavage sites close together. This resembles earlier CLE structure predictions (Meng and Feldman, 2010). Rotamer analysis also showed that this conformation brings Arg5 and Asp8 into close proximity to form a salt bridge, potentially increasing the stability of the mature peptide (Fig. 5B). Surface hydrophobicity analysis suggested that one surface of this structure bulges and is predominantly basic, owing to Arg5, while the opposite surface is uncharged and has a cavity (Fig. 5C). These two surfaces could be involved in binding to receptors. The flanking

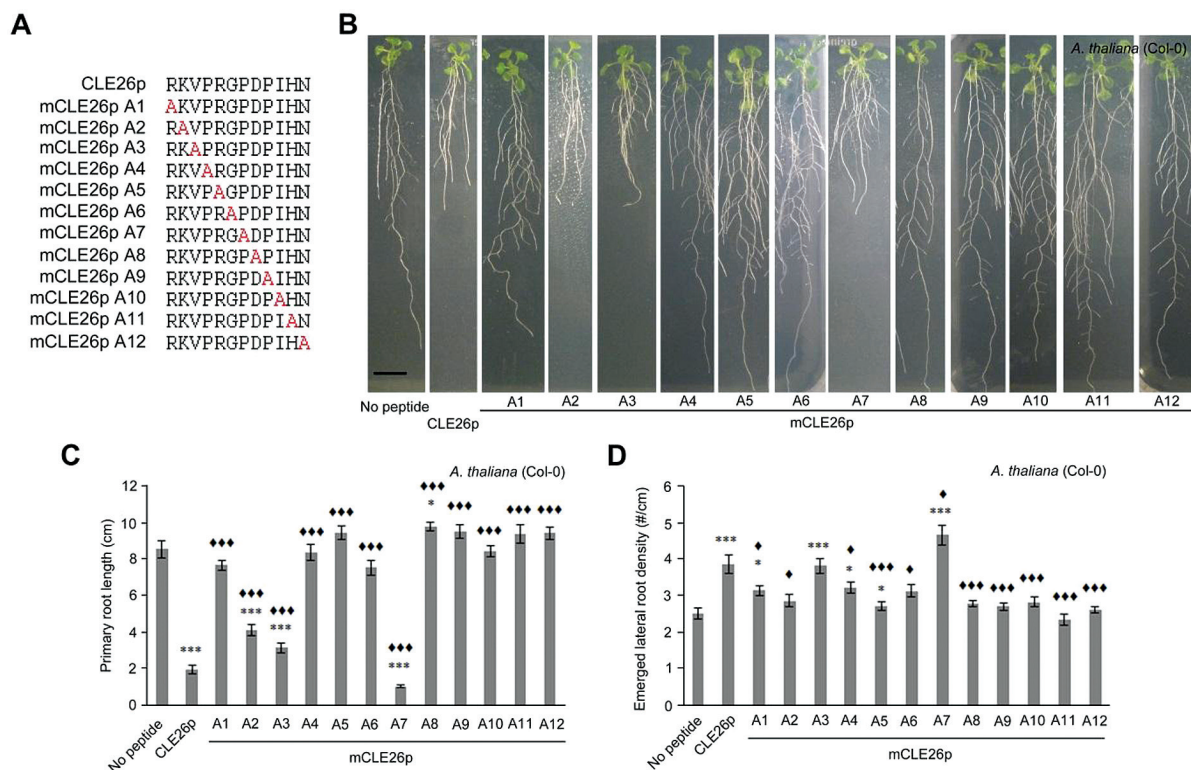


Fig. 4. CLE26p alanine scanning on *A. thaliana*. (A) Sequence of synthetic CLE peptides used. (B) Representative pictures of mCLE26p-treated wild-type seedlings at 12 d after germination. (C, D) Quantification of primary root length (C) and emerged lateral root density (D) for mCLE26p-treated wild-type seedlings. The bar graphs indicate the mean \pm SE. Statistical significance (Student's *t*-test) compared with no peptide (*) and to CLEp treatment (◆) is indicated: ***/◆◆◆ $P < 0.001$, */◆ $P < 0.05$. Scale bar = 1 cm. (This figure is available in colour at *JXB* online.)

precursor sequences are predicted to be α -helices, which may interact prior to mature peptide cleavage, facilitating the formation of a hairpin, and one of these could be membrane associated (Supplementary Fig. S7 at *JXB* online). It has been shown that CLV3p is hydroxylated on each of its proline residues and that the proline at position 7 in the CLV3 peptide is also arabinosylated, enhancing binding to CLV1 and CLV2 (Kondo *et al.*, 2006; Ohyama *et al.*, 2009; Shinohara and Matsubayashi, 2013). CLE26p also contains a proline residue at position 7, and it is worth noting that hydroxyl and arabinose side chains would point towards the arginine–aspartate surface noted above, perturbing their positions slightly (Fig. 5B). Similar modifications in CLE26p might be mimicked by mCLE26p^{P7A}, potentially increasing binding affinity for its orphan receptor and explaining the enhanced biological activity. Indeed, the mCLE26p^{P7A} effect could be mimicked by using a CLE26p variant that is hydroxylated at position 7 (CLE26p^{P7HyP}) (Fig. 5D,E). The alanine at position 7 allows more flexibility in the arms of the hairpin, potentially enabling the arginine–aspartate surface to adopt a more favourable conformation for binding. Molecular dynamics studies of β -1,2-linked tri-arabinosylated CLV3p^{P7} suggest that the effect of the trisaccharide is to bring the N- and C-terminal ends of the peptide closer together (Shinohara and Matsubayashi, 2013), making it more like the hairpin model of CLE26.

The PXPXP motif is conserved in most CLE peptides (Ito *et al.*, 2006), further indicating that formation of a bent hairpin structure is probably important for ligand–receptor interactions. Interestingly the highly conserved proline at position 7 is not critical for bioactivity of TDIF, CLV3, or

CLE26. It is possible that the proline to alanine amino acid exchange at position 7 does not affect the peptide structure and thus does not affect activity, or that this conserved proline at position 7 is a target for post-translational modifications to ‘fine-tune’ the bioactivity of CLE peptides.

AtCLE26p affects Brachypodium and wheat root architecture

To investigate whether the effect of CLE26p observed in *A. thaliana* also extends to monocots, the primary root length of CLE26p-treated *B. distachyon* (Bd21) and wheat was analysed. CLE26p treatment of *B. distachyon* and wheat resulted in a short primary root compared with the untreated control (Fig. 6A–C). These results were similar to those in *A. thaliana* and suggested that an orthologue of *AtCLE26* may also be involved in regulating primary root growth in monocots. However, in contrast to *A. thaliana*, CLE26p application failed to induce any obvious change to lateral root density in *B. distachyon* (Fig. 6D).

To explore CLE26 orthologues in monocots, CLE proteins were searched for in *Z. mays*, *O. sativa* and *B. distachyon*. A WebLogo alignment of mature peptide sequences from *A. thaliana* and *B. distachyon* indicated that mature CLE sequences are highly conserved, both within and between species (Fig. 7A, B). Phylogenetic analyses and sequence alignments indicated that *A. thaliana* mature CLE25 and CLE26 peptides are very similar and only differed at position 5 (asparagine and arginine, respectively) (Fig. 7C, D). While the CLE25p sequence appeared to be fully conserved

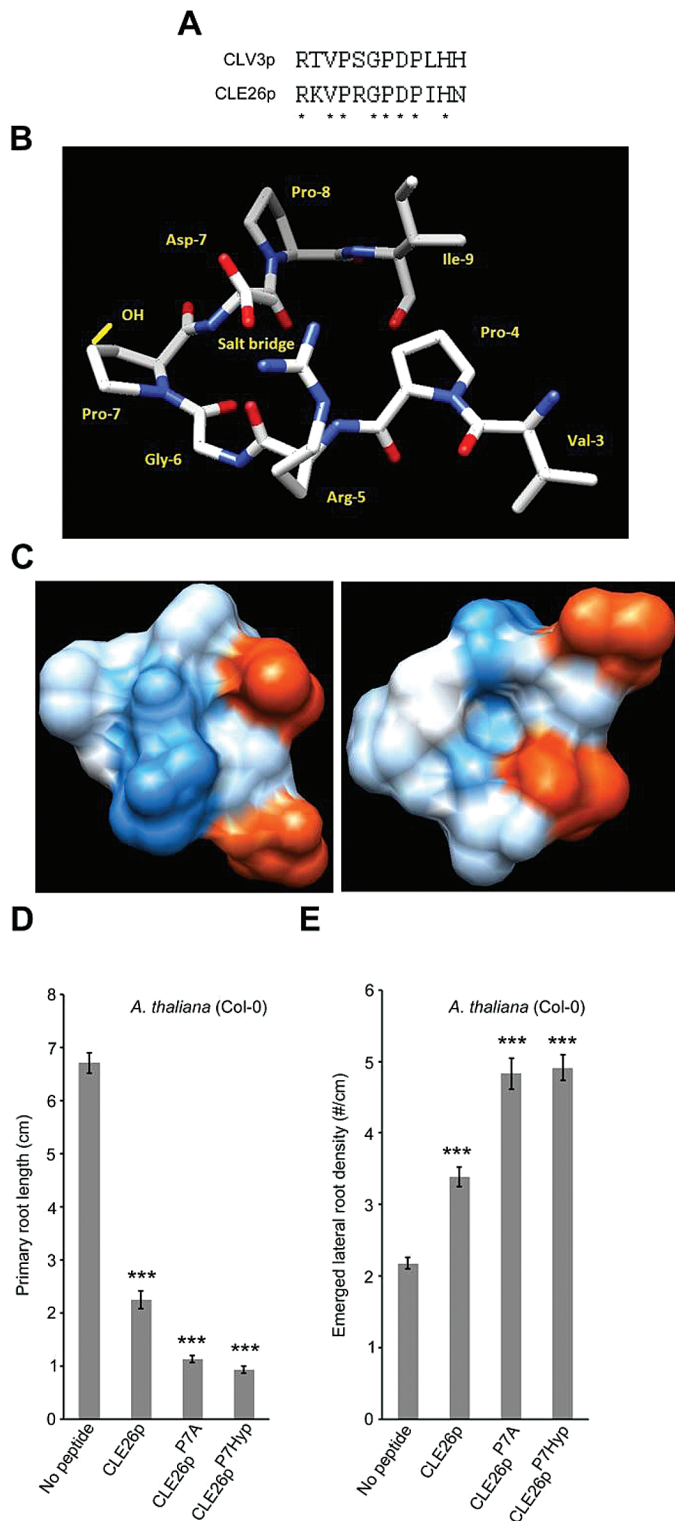


Fig. 5. Sequence and structure versus activity of CLE26p. (A) Conserved residues between CLE26p and CLV3p are denoted by asterisks. (B) The top-ranked predicted structure with amino acids of the cleaved CLE26 peptide named, the position of a potentially stabilizing salt bridge marked, and the hydroxyl group of Pro-7-Hyp (in the 2S, 4S conformation reported from other studies) depicted in yellow. (C) The solvent-accessible surface (left) and solvent-accessible surface of the opposite face of the peptide in (B) (right) coloured in shades of red or blue to indicate the level of acidity or alkalinity, respectively. (D, E) Quantification of primary root length (D) and emerged lateral root density (E) for CLE26p, CLE27p^{P7A} (~mCLE26p A7), and CLE26p^{7Hyp}-treated wild-type seedlings. The graph indicates the mean \pm SE. Statistical significance (Student's *t*-test) compared with no peptide treatment is indicated: ****P*<0.01.

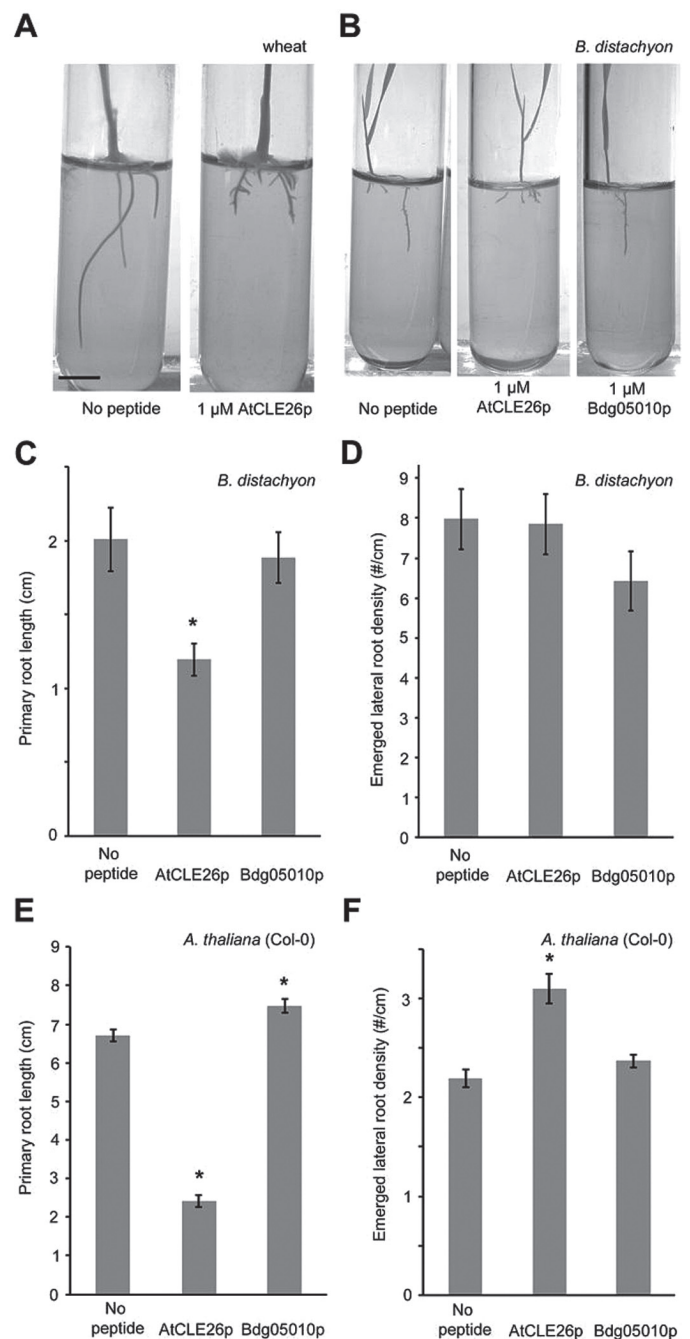


Fig. 6. Effect of AtCLE26p and BdgCLE26p on wheat, *B. distachyon*, and *A. thaliana*. (A, B) Representative pictures are shown for wheat (A) and *B. distachyon* (B) at 12 d after germination. (C, D) Quantification of *B. distachyon* seedling primary root length (C) and emerged lateral root density (D). (E, F) Quantification of *A. thaliana* seedling primary root length (E) and emerged lateral root density (F). The bar graphs indicate the mean \pm SE. Statistical significance (Student's *t*-test) compared with no peptide treatment is indicated: ****P*<0.01. Scale bar = 1 cm.

in monocots such as rice and maize, completely conserved CLE26p sequences were not retrieved (Fig. 7C, E). Putative CLE26p-like sequences differed at one or two positions, namely position 2 (arginine instead of lysine) and 5 (asparagine instead of arginine) in *B. distachyon*, *Z. mays* and *O. sativa* (Fig. 7E). According to the blocks substitution matrix 62 (BLOSUM62), these substitutions are conservative amino acid substitutions—the substitution has similar biochemical properties to that of the original—and should,

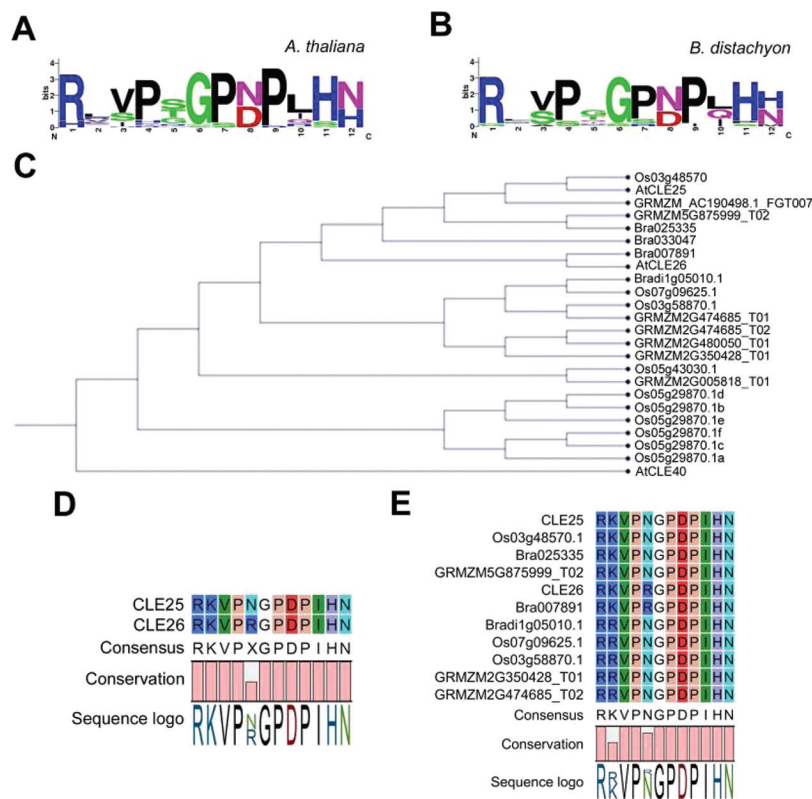


Fig. 7. Phylogenetic analysis of mature CLE25 and CLE26 orthologues. (A, B) Weblogo for *A. thaliana* (A) and *B. distachyon* mature CLE peptide sequences (B). (C) Phylogenetic tree. (D-E) Alignment of the indicated CLE peptide sequences in *Arabidopsis thaliana*, *Oryza sativa* (Os), *Brassica rapa* (Bra), *Zea mays* (GRMZM), and *Brachypodium distachyon* (Bradi). (This figure is available in colour at JXB online.)

therefore, not strongly affect the bioactivity of the peptide. However, the CLE26p alanine scan showed that the arginine at position 5 was essential for function in *A. thaliana*, while the lysine at position 2 was not (Fig. 4). Based on these observations, it cannot be ruled out that a non-specific CLE26p effect was observed in wheat and *B. distachyon*. To investigate this further, a synthetic CLEp derived from a *B. distachyon* *Bradi1g05010*-encoded protein (Bd1g05010p), a CLE25p/CLE26p-related CLE peptide, was applied to *A. thaliana* seedlings. This did not recapitulate the effects observed for the *A. thaliana* CLE26p (Fig. 6E, F), indeed supporting that this peptide is not active in *A. thaliana*. In contrast, Bd1g05010p-treated *A. thaliana* seedlings display a slightly increased primary root length (Fig. 6E), suggesting that Bd1g05010p might act as an antagonistic peptide. Next, Bd1g05010p was applied to *B. distachyon* and the impact on root architecture was evaluated. Interestingly, Bd1g05010p did not reduce primary root length, but slightly decreased lateral root density (Fig. 6C, D). This is opposite to what was observed with the *A. thaliana* CLE26p and to what was previously observed for *A. thaliana* CLE25p (Strabala et al., 2006; Kinoshita et al., 2007). It appears that the change of the conserved amino acid K into R has a strong impact on functionality. While this needs to be explored in more detail, the monocot Bd1g05010p is possibly not a functional orthologue of *A. thaliana* CLE26p or even CLE25p. This may indicate the presence of another (currently unknown) peptide present in *B. distachyon*, which, although less similar in primary sequence to *A. thaliana* CLE26p, is able to form a

similar secondary structure, fulfilling the role of CLE26 role in *B. distachyon*.

CLE26 peptide affects auxin response

Since auxin plays a dominant role in primary root growth and lateral root initiation and development (De Smet, 2012; Lavenus et al., 2013; Tian et al., 2014), it was explored whether and potentially where CLE26p would have an influence on auxin response. For this, it was first tested if *CLE26* expression was regulated by auxin. qPCR analyses showed an ~4-fold increase in *CLE26* expression in wild-type seedling roots following 6 h of auxin treatment (Fig. 8A). Subsequently, it was tested whether CLE26p affects the auxin response marker *pDR5::GUS*. At 1 nM CLE26p, a concentration that significantly affected primary root growth, no obvious difference in *pDR5::GUS* expression was observed in the primary root tip (Fig. 8B). However, at a higher concentration (1 μ M), the *pDR5::GUS* expression level was significantly reduced (Fig. 8B). Subsequently, the AUX/IAA protein-based auxin sensor *p35S::DII:VENUS* (Vernoux et al., 2011; Brunoud et al., 2012) was tested upon CLE26p treatment. While a mild increase in DII:VENUS fluorescence was observed at 1 nM CLE26p, there was a dramatic increase at 1 μ M (Fig. 8C). In agreement with the *pDR5::GUS* results (Fig. 8B), this suggested an altered auxin response in the root tip. These observations are similar to what was recently observed using 10 nM CLE26p on *pDR5::NLS-3xVENUS* for 48 h (Rodriguez-Villalon et al., 2015). Next, to determine if the effect of CLE26p on the auxin response and/or distribution

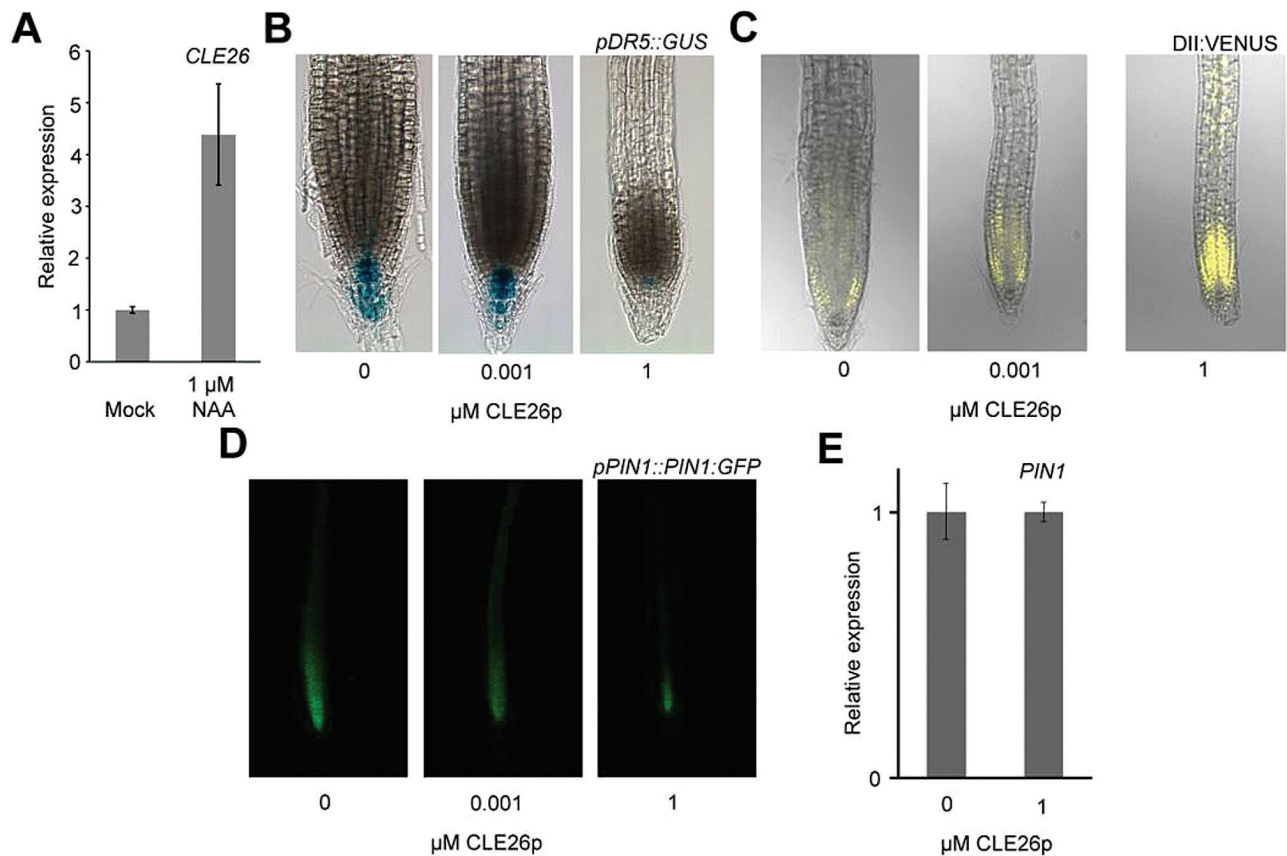


Fig. 8. CLE26 and auxin response/transport. (A) *CLE26* expression level as determined by qPCR in auxin-treated (6 h) 5-day-old wild-type seedlings. (B–D) CLE26p-treated *pDR5::GUS* (B), *35S::DII::VENUS* (C), and *pPIN1::PIN1::GFP* 5-day-old seedlings continuously grown on CLE26p (D). (E) *PIN1* expression level in 7-day-old seedling roots treated with CLE26p for 24 h. The bar graph indicates the mean \pm SE.

in the root tip could be related to CLE26p regulation of polar auxin transport, the *pPIN1::PIN1::GFP* marker line was used (Benková *et al.*, 2003). The *pPIN1::PIN1::GFP* marker displayed mildly and strongly reduced fluorescence at 1 nM and 1 μ M, respectively (Fig. 8D; Supplementary Fig. S8 at JXB online). An even stronger effect on PIN1 fluorescence and localization was observed with 1 nM CLE26p^{P7HyP} (Supplementary Fig. S8). However, this reduction is in contrast to the qPCR results, where CLE26p treatment did not dramatically affect *PIN1* expression in the root (Fig. 8E). This suggested a possible CLE26p-mediated effect on PIN1:GFP at the protein level, which could explain the reduced auxin response in the root tip.

Finally, it was analysed whether CLE26p acts upstream or downstream of the ARF7–ARF19 module, a major regulator of lateral root development (Lavenus *et al.*, 2013). For this, the impact of CLE26p treatment on *ARF7* and *ARF19* expression was tested using qPCR. In CLE26p-treated roots, the *ARF7* and *ARF19* expression levels are not significantly affected (Fig. 9A). Subsequently, the effect of CLE26p treatment on *arf7arf19* was tested. Interestingly, the lateral rootless *arf7arf19* double mutant was partially insensitive to CLE26p with respect to primary root length, but displayed a limited—often closely grouped—number of lateral roots upon CLE26p treatment (Fig. 9B–E). In conclusion, on the one hand, CLE26p appears to require an ARF7- and ARF19-dependent auxin response for its activity, but, on the other hand, it appears to be able to induce lateral root development

in *arf7arf19*. These two—seemingly opposing—effects can possibly be reconciled through a CLE26-mediated perturbation of auxin transport and accumulation.

An Arabidopsis *cle26* mutant affects root architecture

To explore further the role of CLE26 in mediating root architecture, a T-DNA insertion line, which was named *cle26-1*, was analysed (Fig. 10A). Interestingly, *CLE26* has two splicing variants that are both expressed in the root (Fig. 10A; Supplementary Fig. S9 at JXB online). qPCR was performed to examine *CLE26* mRNA transcript levels (using a primer pair that captures both *CLE26.1* and *CLE26.2*) in *cle26-1*, and an ~80% decrease in *CLE26* expression was observed (Fig. 10B). Then the primary root length and lateral root density of *cle26-1* were analysed. This revealed a mild, significant increase with respect to primary root length, and no difference in the level of emerged lateral root density (Fig. 10C–E). Overall, it appears that CLE26 impacts on primary root length and that its effect on lateral root density may be compensated for by other closely related signalling pathways or by genetic redundancy with other CLE peptides.

Conclusion

Taken together, the gain- and loss-of-function data support a role for CLE26 in regulating root architecture. It was

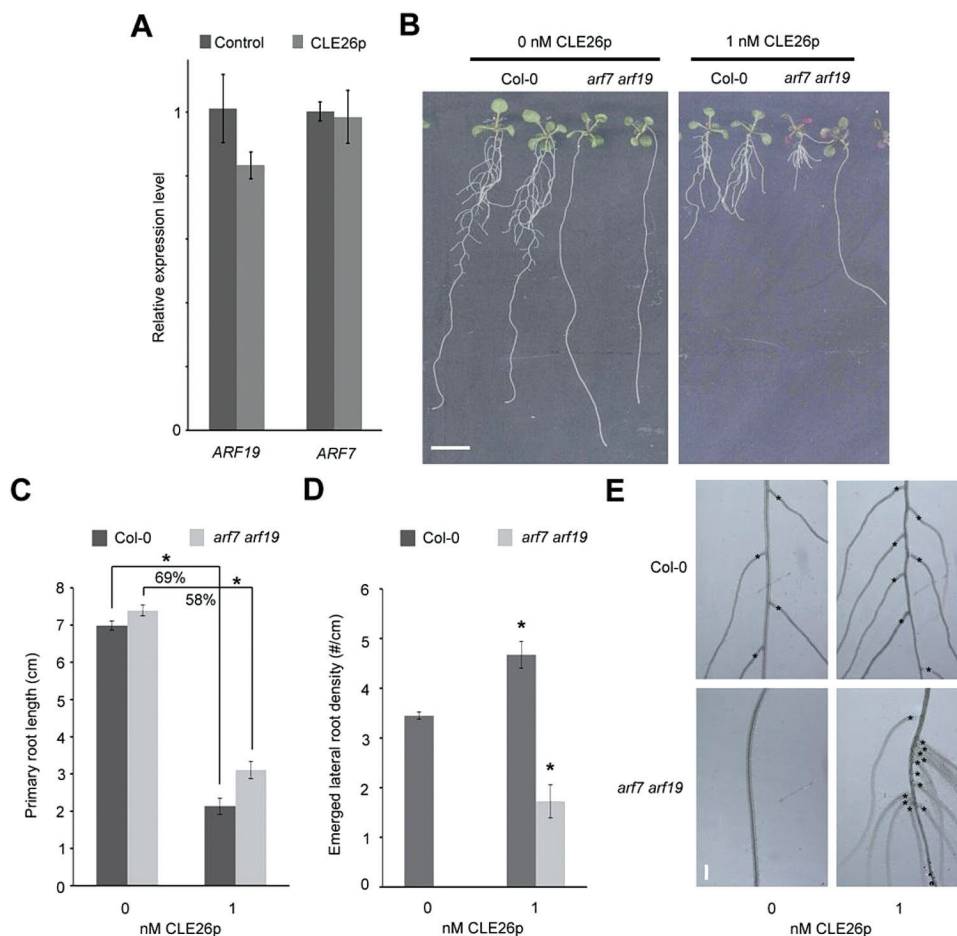


Fig. 9. CLE26p and ARF7–ARF19. (A) *ARF7* and *ARF19* expression as determined by qPCR in 7-day-old seedling roots treated with 1 μ M CLE26p for 24 h. The bar graph indicates the mean \pm SE. (B–E) Root phenotype of CLE26p-treated Col-0 and *arf7arf19* at 9 d after germination. Representative pictures (B) and quantification of primary root length (C) and emerged lateral root density (D). The bar graphs indicate the mean \pm SE. Statistical significance (Student's *t*-test) compared with no peptide treatment: **P*<0.05. Scale bar=1 cm (B) and 100 μ m (E). (E) Detail of lateral root positions (asterisk) and density in Col-0 and *arf7arf19* following peptide treatment. (This figure is available in colour at JXB online.)

recently reported that both CLE45 and CLE26 affect primary root protophloem differentiation, which in turn systemically affects root branching (Rodríguez-Villalon *et al.*, 2014, 2015). The present results on CLE26 confirm, and are complementary to, these recently published data on the CLE26 expression pattern and the CLE26p effect on auxin response and *Arabidopsis* root system architecture. The findings indicate that application of CLE26p decreases the distribution of auxin to the root apical meristem, seemingly by decreasing the abundance of PIN1 through post-translational regulation. Interestingly, it has been reported that localization of PIN1 is responsive to cytokinin signalling (Bishopp *et al.*, 2011). Since CLE14 and CLE20 have previously been demonstrated to be cytokinin responsive (Meng and Feldman, 2010), it will be of interest to determine whether CLE26 interacts with cytokinin signalling, which may indicate a role for CLE26 in mediating localization and/or degradation of PIN1 in response to cytokinin (Marhavy *et al.*, 2014). However, it is also possible that altered CLE26-mediated protophloem differentiation globally affects shoot to root transport and/or protein localization, including PIN1-mediated auxin distribution, but also, for example, the distribution of sugars.

On a structural level, the alanine scanning data indicated a hyperactive proline (CLE26^{P7}). Further analysis indicated that the mCLE26p^{P7A} variant mimics the effect on bioactivity of CLE26p^{P7Hyp}. The former could affect the position of the arms of the loop, while the latter could achieve the same effect by altering the positions of Arg5 and Asp8. The CLE26 model also suggests that other interactions between amino acids may contribute to the folding process, and thus the bioactivity of CLE26p. In view of a possible antagonistic peptide, a new approach to obtain loss-of-function phenotypes that has, however, some limitations (Song *et al.*, 2013; Czyzewicz *et al.*, 2015), mCLE26p^{D8A} has some potential as it appears to mimic the *cle26-1* phenotype.

In monocot model systems (*Brachypodium* and wheat), synthetic CLE26 application exhibited a similar reduction in primary root length, suggesting an orthologous signalling pathway. However, application of a sequentially orthologous peptide (termed Bd1g05010p) to *Brachypodium* did not induce a short-root phenotype. This suggests that *Brachypodium* may have evolved a separate signalling peptide to fulfil the same role as CLE26, that, although less similar in primary sequence, presumably forms a similar functional secondary structure. Similarly,

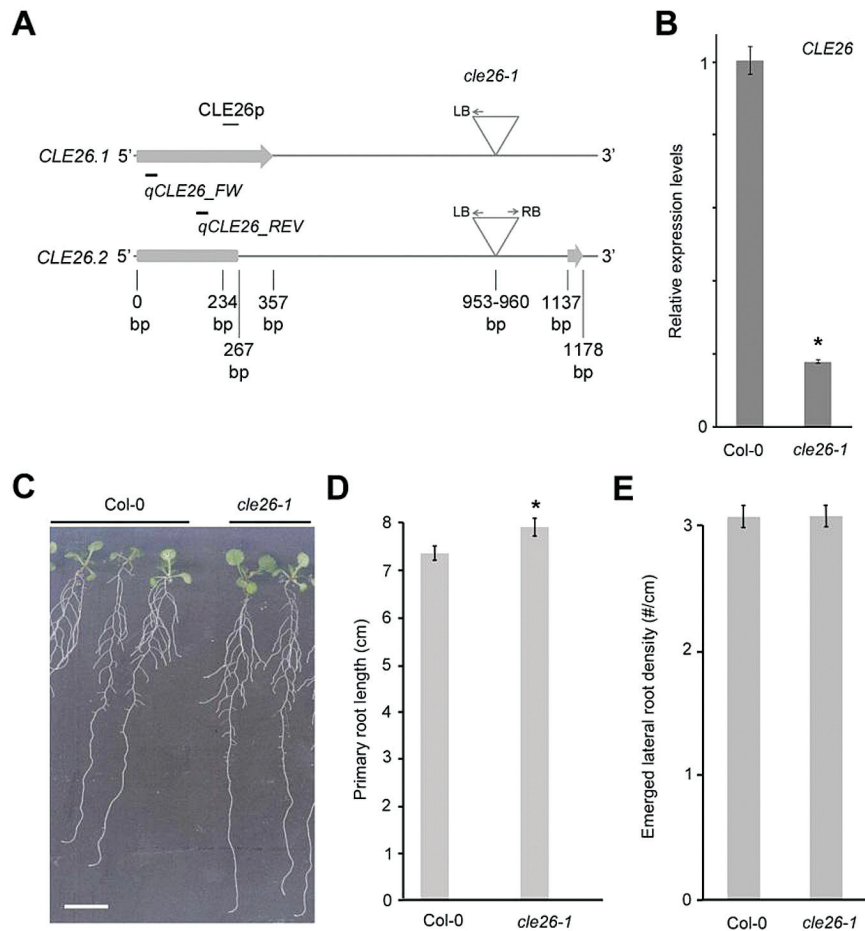


Fig. 10. Characterization of the *cle26-1* mutant. (A) Position of the T-DNA insertion in two splicing variants. Primers used in qPCR are indicated. (B) *CLE26* expression level as determined by qPCR in *cle26-1* roots. (C–E) Root phenotype of *cle26-1* at 9 d after germination. Representative pictures of wild-type and *cle26-1* seedlings (C). (D, E) Quantification of primary root length (D) and emerged lateral root density (E) for *cle26-1* seedlings. The graphs indicate the mean \pm SE. Statistical significance (Student's *t*-test) compared with Col-0 is indicated: * $P < 0.05$. Scale bar = 1 cm. (This figure is available in colour at *JXB* online.)

synthetic Bd1g05010p did not induce a short-root phenotype when applied to *Arabidopsis* at the same concentration as AtCLE26p, indicating that the peptide is either non-functional, or requires a higher concentration in order to stimulate its receptor in both species.

Supplementary data

Supplementary data are available at *JXB* online.

Figure S1. *pCLE::GUS* expression in *Arabidopsis* primary root tip.

Figure S2. *pCLE::GUS* expression during early stages of *Arabidopsis* lateral root development.

Figure S3. *pCLE::GUS* expression during later stages of *Arabidopsis* lateral root development.

Figure S4. *pCLE::GUS* expression in selected stages of lateral root development.

Figure S5. Emerged lateral root numbers corresponding to Figs 2D, E, and 4D.

Figure S6. CLE26p effect on *pAT2G18380::GFP* in primary root tip.

Figure S7. CLE26 consensus secondary structure prediction.

Figure S8. CLE26p effect on PIN1:GFP.

Figure S9. *CLE26* splicing variants in the root.

Figure S10. PSI-BLAST output for CLE26.

Table S1. *pCLE::GUS* lines.

Acknowledgements

We thank Jennifer Fletcher, Anthony Bishopp, and the NASC for providing seeds, and Ruth Cornock and Stephanie Smith for technical support. This work was supported by a BBSRC David Phillips Fellowship (BB_BB/H022457/1) and a Marie Curie European Reintegration Grant (PERG06-GA-2009-256354) to IDS, a BBSRC CASE Studentship co-funded by Bayer CropScience to NC, and grants 13785/F20 and 230849/F20 to MAB, and 348256/F20 to C-LS from the Research Council of Norway. LDV received a VIB International PhD Scholarship in life sciences.

References

- Araya T, Miyamoto M, Wibowo J, *et al.* 2014. CLE–CLAVATA1 peptide–receptor signaling module regulates the expansion of plant root systems in a nitrogen-dependent manner. *Proceedings of the National Academy of Sciences, USA* **111**, 2029–2034.
- Benková E, Michniewicz M, Sauer M, Teichmann T, Seifertová D, Jürgens G, Friml J. 2003. Local, efflux-dependent auxin gradients as a common module for plant organ formation. *Cell* **115**, 591–602.
- Betsuyaku S, Sawa S, Yamada M. 2011. The function of the CLE peptides in plant development and plant–microbe interactions. *Arabidopsis Book* **9**, e0149.

- Bidadi H, Matsuoka K, Sage-Ono K, et al.** 2014. CLE6 expression recovers gibberellin deficiency to promote shoot growth in Arabidopsis. *The Plant Journal* **78**, 241–252.
- Bishopp A, Help H, El-Showk S, Weijers D, Scheres B, Friml J, Benková E, Mähönen Ari P, Helariutta Y.** 2011. A mutually inhibitory interaction between auxin and cytokinin specifies vascular pattern in roots. *Current Biology* **21**, 917–926.
- Brunoud G, Wells DM, Oliva M, et al.** 2012. A novel sensor to map auxin response and distribution at high spatio-temporal resolution. *Nature* **482**, 103–106.
- Butenko MA, Vie AK, Brembu T, Aalen RB, Bones AM.** 2009. Plant peptides in signalling: looking for new partners. *Trends in Plant Science* **14**, 255–263.
- Butenko MA, Wildhagen M, Albert M, Jehle A, Kalbacher H, Aalen RB, Felix G.** 2014. Tools and strategies to match peptide–ligand receptor pairs. *The Plant Cell* **26**, 1838–1847.
- Casamitjana-Martinez E, Hofhuis HF, Xu J, Liu CM, Heidstra R, Scheres B.** 2003. Root-specific CLE19 overexpression and the *sol1/2* suppressors implicate a CLV-like pathway in the control of Arabidopsis root meristem maintenance. *Current Biology* **13**, 1435–1441.
- Clark SE, Running MP, Meyerowitz EM.** 1995. CLAVATA3 is a specific regulator of shoot and floral meristem development affecting the same processes as CLAVATA1. *Development* **121**, 2057–2067.
- Crooks GE, Hon G, Chandonia JM, Brenner SE.** 2004. WebLogo: a sequence logo generator. *Genome Research* **14**, 1188–1190.
- Czyzewicz N, Wildhagen M, Cattaneo P, et al.** 2015. Antagonistic peptide technology revisited. *Journal of Experimental Biology* **66**, 5367–5374.
- Czyzewicz N, Yue K, Beeckman T, De Smet I.** 2013. Message in a bottle: small signalling peptide outputs during growth and development. *Journal of Experimental Biology* **64**, 5281–5296.
- Davière J-M, Achard P.** 2013. Gibberellin signaling in plants. *Development* **140**, 1147–1151.
- Depuydt S, Rodriguez-Villalón A, Santuari L, Wyser-Rmili C, Ragni L, Hardtke CS.** 2013. Suppression of Arabidopsis protophloem differentiation and root meristem growth by CLE45 requires the receptor-like kinase BAM3. *Proceedings of the National Academy of Sciences, USA* **110**, 7074–7079.
- De Smet I.** 2012. Lateral root initiation: one step at a time. *New Phytologist* **193**, 867–873.
- De Smet I, Signora L, Beeckman T, Inze D, Foyer CH, Zhang H.** 2003. An abscisic acid-sensitive checkpoint in lateral root development of Arabidopsis. *The Plant Journal* **33**, 543–555.
- De Smet I, Tetsumura T, De Rybel B, et al.** 2007. Auxin-dependent regulation of lateral root positioning in the basal meristem of Arabidopsis. *Development* **134**, 681–690.
- Ding Z, De Smet I.** 2013. Localised ABA signalling mediates root growth plasticity. *Trends in Plant Science* **18**, 533–535.
- Duan L, Dietrich D, Ng CH, Chan PM, Bhalerao R, Bennett MJ, Dinneny JR.** 2013. Endodermal ABA signaling promotes lateral root quiescence during salt stress in Arabidopsis seedlings. *The Plant Cell* **25**, 324–341.
- Dunbrack RL Jr.** 2002. Rotamer libraries in the 21st century. *Current Opinion in Structural Biology* **12**, 431–440.
- El-Showk S, Ruonala R, Helariutta Y.** 2013. Crossing paths: cytokinin signalling and crosstalk. *Development* **140**, 1373–1383.
- Fiers M, Golemic E, Xu J, van der Geest L, Heidstra R, Stiekema W, Liu CM.** 2005. The 14-amino acid CLV3, CLE19, and CLE40 peptides trigger consumption of the root meristem in Arabidopsis through a CLAVATA2-dependent pathway. *The Plant Cell* **17**, 2542–2553.
- Fletcher JC, Brand U, Running MP, Simon R, Meyerowitz EM.** 1999. Signaling of cell fate decisions by CLAVATA3 in Arabidopsis shoot meristems. *Science* **283**, 1911–1914.
- Funayama-Noguchi S, Noguchi K, Yoshida C, Kawaguchi M.** 2011. Two CLE genes are induced by phosphate in roots of *Lotus japonicus*. *Journal of Plant Research* **124**, 155–163.
- Geier F, Lohmann JU, Gerstung M, Maier AT, Timmer J, Fleck C.** 2008. A quantitative and dynamic model for plant stem cell regulation. *PLoS One* **3**, e3553.
- Goodstein DM, Shu S, Howson R, et al.** 2011. Phytozome: a comparative platform for green plant genomics. *Nucleic Acids Research* **40**, D1178–D1186.
- Gruber BD, Giehl RF, Friedel S, von Wiren N.** 2013. Plasticity of the Arabidopsis root system under nutrient deficiencies. *Plant Physiology* **163**, 161–179.
- Guo Y, Han L, Hymes M, Denver R, Clark SE.** 2010. CLAVATA2 forms a distinct CLE-binding receptor complex regulating Arabidopsis stem cell specification. *The Plant Journal* **63**, 889–900.
- Hellemans J, Mortier G, De Paepe A, Speleman F, Vandesompele J.** 2007. qBase relative quantification framework and software for management and automated analysis of real-time quantitative PCR data. *Genome Biology* **8**, R19.
- Hirakawa Y, Shinohara H, Kondo Y, et al.** 2008. Non-cell-autonomous control of vascular stem cell fate by a CLE peptide/receptor system. *Proceedings of the National Academy of Sciences, USA* **105**, 15208–15213.
- Hobe M, Muller R, Grunewald M, Brand U, Simon R.** 2003. Loss of CLE40, a protein functionally equivalent to the stem cell restricting signal CLV3, enhances root waving in Arabidopsis. *Development Genes and Evolution* **213**, 371–381.
- Ito Y, Nakanomyo I, Motose H, Iwamoto K, Sawa S, Dohmae N, Fukuda H.** 2006. Dodeca-CLE peptides as suppressors of plant stem cell differentiation. *Science* **313**, 842–845.
- Jun J, Fiume E, Roeder AHK, et al.** 2010. Comprehensive analysis of CLE polypeptide signaling gene expression and overexpression activity in Arabidopsis. *Plant Physiology* **154**, 1721–1736.
- Kelley LA, Sternberg MJ.** 2009. Protein structure prediction on the Web: a case study using the Phyre server. *Nature Protocols* **4**, 363–371.
- Kinoshita A, Nakamura Y, Sasaki E, Kyozuka J, Fukuda H, Sawa S.** 2007. Gain-of-function phenotypes of chemically synthetic CLAVATA3/ESR-related (CLE) peptides in Arabidopsis thaliana and Oryza sativa. *Plant and Cell Physiology* **48**, 1821–1825.
- Kondo T, Nakamura T, Yokomine K, Sakagami Y.** 2008. Dual assay for MCLV3 activity reveals structure–activity relationship of CLE peptides. *Biochemical and Biophysical Research Communications* **377**, 312–316.
- Kondo T, Sawa S, Kinoshita A, Mizuno S, Kakimoto T, Fukuda H, Sakagami Y.** 2006. A plant peptide encoded by CLV3 identified by *in situ* MALDI-TOF MS analysis. *Science* **313**, 845–848.
- Kurup S, Runions J, Kohler U, Laplace L, Hodge S, Haseloff J.** 2005. Marking cell lineages in living tissues. *The Plant Journal* **42**, 444–453.
- Lavenus J, Goh T, Roberts I, et al.** 2013. Lateral root development in Arabidopsis: fifty shades of auxin. *Trends in Plant Science* **18**, 450–458.
- Lee JY, Colinas J, Wang JY, Mace D, Ohler U, Benfey PN.** 2006. Transcriptional and posttranscriptional regulation of transcription factor expression in Arabidopsis roots. *Proceedings of the National Academy of Sciences, USA* **103**, 6055–6060.
- Lim CW, Lee YW, Lee SC, Hwang CH.** 2014. Nitrate inhibits soybean nodulation by regulating expression of CLE genes. *Plant Science* **229**, 1–9.
- Malamy JE, Benfey PN.** 1997. Organization and cell differentiation in lateral roots of Arabidopsis thaliana. *Development* **124**, 33–44.
- Marhavy P, Duclercq J, Weller B, et al.** 2014. Cytokinin controls polarity of PIN1-dependent auxin transport during lateral root organogenesis. *Current Biology* **24**, 1031–1037.
- Matsubayashi Y.** 2011. Post-translational modifications in secreted peptide hormones in plants. *Plant and Cell Physiology* **52**, 5–13.
- Matsuzaki Y, Ogawa-Ohnishi M, Mori A, Matsubayashi Y.** 2010. Secreted peptide signals required for maintenance of root stem cell niche in Arabidopsis. *Science* **329**, 1065–1067.
- Meng L, Feldman LJ.** 2010. CLE14/CLE20 peptides may interact with CLAVATA2/CORYNE receptor-like kinases to irreversibly inhibit cell division in the root meristem of Arabidopsis. *Planta* **232**, 1061–1074.
- Miyawaki K, Tabata R, Sawa S.** 2013. Evolutionarily conserved CLE peptide signaling in plant development, symbiosis, and parasitism. *Current Opinion in Plant Biology* **16**, 598–606.
- Mortier V, De Wever E, Vuylsteke M, Holsters M, Goormachtig S.** 2012. Nodule numbers are governed by interaction between CLE peptides and cytokinin signaling. *The Plant Journal* **70**, 367–376.
- Murphy E, De Smet I.** 2014. Understanding the RALF family: a tale of many species. *Trends in Plant Science* **19**, 664–671.
- Murphy E, Smith S, De Smet I.** 2012. Small signaling peptides in Arabidopsis development: how cells communicate over a short distance. *The Plant Cell* **24**, 3198–3217.

- Ogawa M, Shinohara H, Sakagami Y, Matsubayashi Y.** 2008. Arabidopsis CLV3 peptide directly binds CLV1 ectodomain. *Science* **319**, 1150083.
- Ohyama K, Shinohara H, Ogawa-Ohnishi M, Matsubayashi Y.** 2009. A glycopeptide regulating stem cell fate in Arabidopsis thaliana. *Nature Chemical Biology* **5**, 578–580.
- Okamoto S, Ohnishi E, Sato S, Takahashi H, Nakazono M, Tabata S, Kawaguchi M.** 2009. Nod factor/nitrate-induced CLE genes that drive HAR1-mediated systemic regulation of nodulation. *Plant and Cell Physiology* **50**, 67–77.
- Okushima Y, Fukaki H, Onoda M, Theologis A, Tasaka M.** 2007. ARF7 and ARF19 regulate lateral root formation via direct activation of LBD/ASL genes in Arabidopsis. *The Plant Cell* **19**, 118–130.
- Parizot B, Laplaze L, Ricaud L, et al.** 2008. Diarch symmetry of the vascular bundle in Arabidopsis root encompasses the pericycle and is reflected in distich lateral root initiation. *Plant Physiology* **146**, 140–148.
- Parizot B, Roberts I, Raes J, Beeckman T, De Smet I.** 2012. In silico analyses of pericycle cell populations reinforce their relation with associated vasculature in Arabidopsis. *Philosophical Transactions of the Royal Society B: Biological Sciences* **367**, 1479–1488.
- Pearce G, Moura DS, Stratmann J, Ryan CA.** 2001. RALF, a 5-kDa ubiquitous polypeptide in plants, arrests root growth and development. *Proceedings of the National Academy of Sciences, USA* **98**, 12843–12847.
- Péret B, De Rybel B, Casimiro I, Benková E, Swarup R, Laplaze L, Beeckman T, Bennett MJ.** 2009. Arabidopsis lateral root development: an emerging story. *Trends in Plant Science* **14**, 399–408.
- Pettersen EF, Goddard TD, Huang CC, Couch GS, Greenblatt DM, Meng EC, Ferrin TE.** 2004. UCSF Chimera—a visualization system for exploratory research and analysis. *Journal of Computational Chemistry* **25**, 1605–1612.
- Reid DE, Ferguson BJ, Gresshoff PM.** 2011. Inoculation- and nitrate-induced CLE peptides of soybean control NARK-dependent nodule formation. *Molecular Plant-Microbe Interactions* **24**, 606–618.
- Rodríguez-Villalón A, Gujas B, Kang YH, Breda AS, Cattaneo P, Depuydt S, Hardtke CS.** 2014. Molecular genetic framework for protophloem formation. *Proceedings of the National Academy of Sciences, USA* **111**, 11551–11556.
- Rodríguez-Villalón A, Gujas B, van Wijk R, Munnik T, Hardtke CS.** 2015. Primary root protophloem differentiation requires balanced phosphatidylinositol-4–5-bisphosphate levels and systemically affects root branching. *Development* **142**, 1437–1446.
- Sawa S, Kinoshita A, Nakanomyo I, Fukuda H.** 2006. CLV3/ESR-related (CLE) peptides as intercellular signaling molecules in plants. *Chemical Record* **6**, 303–310.
- Schindelin J, Arganda-Carreras I, Frise E, et al.** 2012. Fiji: an open-source platform for biological-image analysis. *Nature Methods* **9**, 676–682.
- Sharma V, Ramirez J, Fletcher J.** 2003. The Arabidopsis CLV3-like (CLE) genes are expressed in diverse tissues and encode secreted proteins. *Plant Molecular Biology* **51**, 415–425.
- Shinohara H, Matsubayashi Y.** 2013. Chemical synthesis of Arabidopsis CLV3 glycopeptide reveals the impact of hydroxyproline arabinosylation on peptide conformation and activity. *Plant and Cell Physiology* **54**, 369–374.
- Smith S, De Smet I.** 2012. Root system architecture: insights from Arabidopsis and cereal crops. *Philosophical Transactions of the Royal Society B: Biological Sciences* **367**, 1441–1452.
- Song XF, Guo P, Ren SC, Xu TT, Liu CM.** 2013. Antagonistic peptide technology for functional dissection of CLV3/ESR genes in Arabidopsis. *Plant Physiology* **161**, 1076–1085.
- Stahl Y, Grabowski S, Bleckmann A, et al.** 2013. Moderation of Arabidopsis root stemness by CLAVATA1 and ARABIDOPSIS CRINKLY4 receptor kinase complexes. *Current Biology* **23**, 362–371.
- Strabala TJ, O'Donnell PJ, Smit A-M, et al.** 2006. Gain-of-function phenotypes of many CLAVATA3/ESR genes, including four new family members, correlate with tandem variations in the conserved CLAVATA3/ESR domain. *Plant Physiology* **140**, 1331–1344.
- Tian H, De Smet I, Ding Z.** 2014. Shaping a root system: regulating lateral versus primary root growth. *Trends in Plant Science* **19**, 426–431.
- Vanstraelen M, Benkova E.** 2012. Hormonal interactions in the regulation of plant development. *Annual Review of Cell and Developmental Biology* **28**, 463–487.
- Vernoux T, Brunoud G, Farcot E, et al.** 2011. The auxin signalling network translates dynamic input into robust patterning at the shoot apex. *Molecular Systems Biology* **7**, 508.
- Wang G, Fiers M.** 2010. CLE peptide signaling during plant development. *Protoplasma* **240**, 33–43.
- Yoon GM, Kieber JJ.** 2013. 1-Aminocyclopropane-1-carboxylic acid as a signalling molecule in plants. *AoB Plants* **5**, plt017.
- Zhao C, Craig JC, Petzold HE, Dickerman AW, Beers EP.** 2005. The xylem and phloem transcriptomes from secondary tissues of the Arabidopsis root-hypocotyl. *Plant Physiology* **138**, 803–818.